Wear 524-525 (2023) 204804

Contents lists available at ScienceDirect

Wear

journal homepage: www.elsevier.com/locate/wear

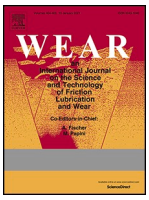

Galling of stainless steels as a function of test conditions in an ASTM G196-type test setup – The role of temperature, rotational velocity, interrupted rotation and rotational distance

J.L. Daure [a,*], D. Kóti [a], M.J. Carrington [a], D.G. McCartney [a], D.A. Stewart [b], P.H. Shipway [a]

[a] Faculty of Engineering, University of Nottingham, UK
[b] Rolls-Royce Plc, Derby, UK

A B S T R A C T

Austenitic stainless steels have attractive properties for use in corrosive environments, but their use in components where motion under load is experienced (such as valves) is limited by their poor galling behaviour. Whilst stainless steels with improved performance have been developed over many years, the basic understanding of the key parameters in galling of standard stainless steels is not well understood. In this work, the galling behaviour of a dissimilar austenitic stainless steel pair is explored via testing in an instrumented ASTM G196-type test. Key variables examined are environmental temperature (room temperature and 100 °C), rotational speed (2.1 rpm and 5.5 rpm), and the sliding distance (from a quarter of a turn up to five turns). Galling was observed to become more severe with increased temperature, but was not significantly affected by either sliding speed (in the range examined) or interruptions during the rotation. The measurement of friction coefficient along with surface observations revealed that galling does not take place within the initial period of sliding; however, damage is being accrued by the sample surfaces which then results in subsequent observable galling as the sliding distance is increased. The importance of measuring torque during galling tests is illustrated, and the findings provide useful information with regard to those test variables that require critical control (and which do not) during conduct of a galling test programme.

1. Introduction

Galling is a particularly aggressive form of plasticity-dominated wear in which subsurface plastic deformation becomes unstable leading to abrupt macroscale damage and surface failure [1]. The complete failure of a surface via galling is inherently transient in nature; this is in contrast to other milder forms of plasticity dominated wear, for example, scuffing and adhesive wear regimes, where surface degradation and failure generally have a steady state period of more predictable surface damage and material removal during continued sliding contact [2]. Nevertheless, galling is typically characterized by macroscopic roughening of the surfaces and transfer or displacement of large fragments of material which form visible protrusions on the original surfaces [2,3]. Galling is a concern as it often results in the abrupt failure of components and mechanisms due to binding or seizure of mated components which are required to move against each other [4,5], such as threaded fasteners, pin joints and valve faces [6].

A wide variety of galling test methodologies are available, with a summary of these having been presented by Hummel and Helm [4]. The most widely used tests are those described by the ASTM standards G98 (first approved in 1989) [7] and G196 (first approved in 2008) [3], with the development of the G196 test being driven by some of the perceived shortcomings of the G98 test [8]. The G98 test involves the rotation of a solid cylinder around its own axis whilst one circular end is loaded against a plate, whereas the G196 geometry involves two hollow cylinders of the same geometry loaded against each other along their common axis with relative rotation. For both test types, the standards require a single rotation between the specimens to be applied, and both allow the rotation to be interrupted for regripping of the specimen, with this allowance being made since in many test apparatus, the sample rotation is conducted manually. The G98 standard allows the rate of rotation to vary between 3 rpm and 20 rpm, whereas the G196 standard specifies that the rate of rotation is approximately 6 rpm [3,7]. It is however noted that Hummel and Helm state that "*the sliding distance and speed used in … the ASTM G196 test method were chosen for several pragmatic reasons*" [4]. It is recognised that galling is a stochastic process and that under certain test conditions, galling may be observed in some tests whilst it is not seen in others. This understanding has led to statistically based measures of the galling stress, such as the stress at which 50% of tests are expected to gall, termed the G_{50} value [4,8].

The standards do not specifically address the issue of test temperature, although it is generally understood that an increase in temperature

* Corresponding author.
E-mail address: jaimie.daure@nottingham.ac.uk (J.L. Daure).

https://doi.org/10.1016/j.wear.2023.204804
Received 19 September 2022; Received in revised form 16 January 2023; Accepted 17 January 2023
Available online 1 April 2023

of a material tends to promote galling. Via detailed crystal plasticity based modelling work, Poole et al. [9] recently demonstrated that increases in environmental temperature are expected to increase the tendency to gall which is in accord with the body of experimental evidence; for example, Harsha et al. [10] conducted tests based upon the ASTM G196 standard, and reported that the G_{50} value of 316 stainless steel fell from 12 MPa at room temperature to 2 MPa at 300 °C.

Whilst the rotational speed employed in the test will affect the frictional power input into the contact, Poole et al. [9] have argued that at speeds typical of the galling tests being considered, friction-induced heat generation does not affect the galling behaviour of a 316 stainless steel, since the rate of heat transfer away from the surface far exceeds that of its generation. However, it is noted that this conclusion does not apply to all tests where galling is observed. Higher frictional power densities will be associated with higher contact pressures (due to either higher loads or the smaller contact areas that are often observed with non-conforming contact geometries) or with higher contact sliding speeds, and in these cases, frictional heating may affect the galling behaviour of the materials [11–13]. As such, there is a need to understand the dependence of behaviour upon rotational speed in the ASTM G196 test, and whether the restriction to a single rotational speed (as opposed to the range of rotational speeds allowed in the G98 test) is critical. It is noted that in considering the range of speeds allowed in the ASTM G98 test, Hummel stated [14]: "*Although, to the author's knowledge, a study has not been conducted to quantify the impact of this range of speeds, it is widely understood that the sliding speed effects galling resistance.*" Furthermore, Hummel also indicated a concern related to interruptions in the rotation of samples in the galling tests (allowed in both the G98 and G196 standards), stating: "*The variability in the speed will most certainly adversely impact the galling resistance as will the increase in torque required to overcome the static coefficient of friction at each regripping.*"

Despite the G98 and G196 ASTM standards in this area specifying a single rotation in galling tests, Hummel and Partlow [15] argue (based upon their own work and data from the literature) that as the sliding distance increases, the galling load decreases. The same conclusion is reached in work employing other types of galling test; for example, using the widely used load-scanner type test [16], it has been demonstrated that the load at which galling is deemed to have occurred falls as the sliding distance (or number of passes) increases [17]. These observations imply that damage is accumulated in the contacting surfaces during the pre-galling stage of any test and that most probably galling occurs in response to an unstable evolution of plastic surface damage. This aligns well with numerous studies which directly relate both an instability and increase in friction during sliding to the galling phenomenon [18–20]. These observations suggest that measurement of coefficient of friction during a galling test makes a significant contribution to advancing the current understanding of the galling phenomenon.

In many galling tests, the analysis of whether galling has occurred is made via examination of the surfaces following the test. In some test types, the measurement of friction during the test is commonplace, but in general, measurement of the changes in frictional forces during G98-type and G196-type tests is not conducted; it is noted that the value of torque measurements during testing in identification of incipient scoring is directly addressed in both the G98 and G196 standards, although it is not a requirement of these test standards [3,7]. The measurement of torque during rotary galling tests is not new [21,22] and has been recognised as a key means of understanding the evolution of damage during a test as a supplement to the more widely used post-test analysis of damaged surfaces. Harsha et al. [8,10] measured torque during galling tests of stainless steel with ASTM G196 type specimens at constant rotational speed (6 rpm) and with a total rotation of 720°. In their apparatus, the specimen rotation was mechanised to ensure constant rotational velocity with no interruptions during a test. They reported that in samples where visual inspection revealed galling after testing, a significant increase in the torque was observed at some point during the test. In the data presented, it could be seen that this was typically after at least a rotation of 180° and from this it can be inferred that galling had not occurred in the early part of such tests. In tests where no galling took place, it was notable that a stable frictional torque was observed throughout the tests (i.e. the significant increase in torque seen for the other samples was not observed). Similar observations were made by Hummel [23] who measured torque during a galling test and showed that "*large increases in friction were seen in every test that was performed where galling appeared*" and that the changes could be observed in the torque even in cases where the galling was barely visible.

In the present work, a number of features of the ASTM G196 test specification were explored to understand their role on galling. The test pairing employed is a dissimilar 304–316 stainless steel pair (to facilitate future microstructural examination of mechanisms of damage and galling [24]) with the dependence of galling load on the following parameters being explored: (i) environmental temperature; (ii) sliding speed; (iii) interruptions during sliding; (iv) sliding distance.

2. Experimental procedure

2.1. Description of galling test rig

A test rig has been developed at the University of Nottingham in order to carry out galling tests broadly based upon the ASTM G196 (Standard Test Method for Galling Resistance of Material Couples) configuration [3]. This test rig has been described previously [25] and so only key elements of it will be repeated here.

This method consists of two concentric hollow cylindrical specimens with their ends mated resulting in a contact area in the shape of an annulus. An alignment pin is located in the centre hole of the samples to ensure concentricity between the two specimens throughout the test. A schematic diagram of the test configuration is presented in Fig. 1.

A cross-sectional diagram of the test rig is presented in Fig. 2. The rig conforms to a die-set configuration; an Instron 5581 universal testing machine was used to apply the normal load which was applied in load-controlled mode. The support columns maintain alignment between the upper and lower sections of the rig. The base of the rig is fixed to the bed of the Instron machine and the upper section is attached to its load cell. In this rig, testing can be conducted up to a maximum normal load of 5

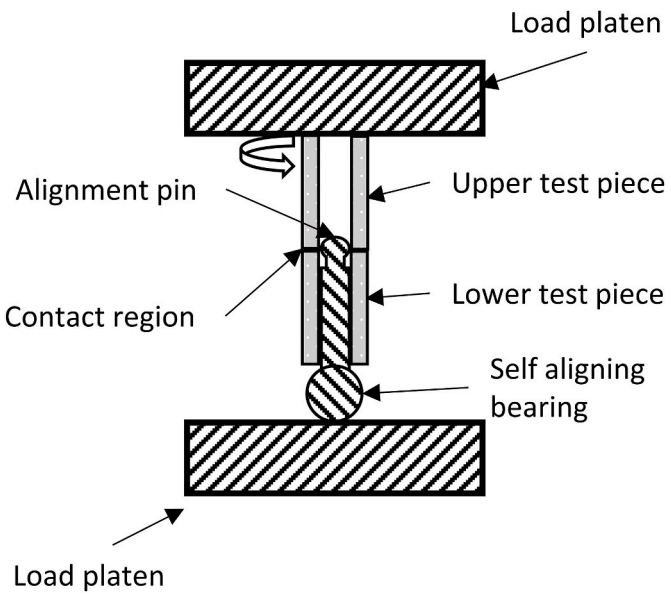

Fig. 1. Schematic diagram showing a cross-sectional view of the test configuration. Loading is applied via the platens, the lower test piece remains stationary whilst the upper test piece is rotated.

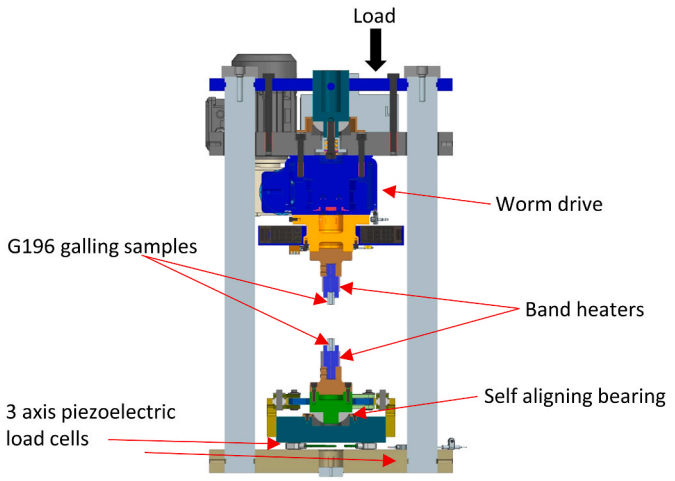

Fig. 2. Schematic diagram showing a cross-sectional view of the of the galling test apparatus.

kN which, under the G196 sample dimensions, equates to a nominal contact pressure of 52.8 MPa. It is noted that this rig has been built to complement one of similar design which has a much higher load capacity and has been previously reported [25].

The use of an automated worm drive to rotate the upper test piece results in a constant and repeatable angular speed and distance for each test. A self-aligning bearing allows the transverse movement and angular displacement of the lower test piece whilst preventing any rotation about the central axis. This mechanism ensures repeatable pin alignment which results in symmetrical load distribution about the axis of rotation at the start of the test. This repeatable uniform loading is of paramount importance to high quality galling testing.

The test pieces are held in a chuck and secured by four grub screws which are screwed onto two flats on the base of the samples at 90° apart. The bottom chuck is fixed to the self-aligning bearing whilst the upper test piece is rotated through a fixed amount per test (90°, 180°, 270° or 360°); these rotations can be either continuous, or with interruptions at any of the defined points. The design of the rig means that for tests that required more than a single rotation, the test pieces are unloaded, rotated back to the start point, and then further rotation is applied as necessary. It is recognised that this results in a disengagement of the test surfaces which may affect the galling behaviour as compared to an uninterrupted test of multiple rotations. The rotation of the test piece is conducted via a variable speed automated worm drive. For this work, the maximum and minimum rotational speeds of 5.5 rpm and 2.1 rpm were employed (rotations of 360° in 11 s and 28 s respectively).

The vertical load and the torque are measured from the output of three 3-axis piezoelectric load cells (Kistler Instruments Ltd.) which are located under the base plate arranged 120° apart; the sensitivity of the load cells is 7.8 pC N^{-1} for the shear force (torque) and 3.8 pC N^{-1} for the normal load. In this work, data were acquired at a sampling rate of 100 Hz.

The rig is situated in an environmentally controlled room where the ambient temperature is maintained at 18 °C. For elevated temperature tests, band heaters with copper bushings surround the test pieces which allow tests to be conducted with a maximum operating temperature of 700 °C. K-type thermocouples are inserted into machined slots in the copper bushings to constantly monitor and control the remote temperature. The temperatures of the surfaces themselves were measured under lightly loaded conditions (<5 MPa) but with no rotational motion. These measured surface temperatures were then correlated with measurements from the remote thermocouples. Thermocouples are not present on the surface during galling tests. This calibration was regularly re-checked to avoid any long-term drift.

2.2. Materials and sample preparation

The materials employed in this study were a 304 austenitic stainless steel (259 ± 11 HV_{20}) and a 316 stainless steel (311 ± 11 HV_{20}) (10 individual Vickers indentations were made for determination of hardness). All galling tests were conducted with a 304 (upper test piece) stainless steel sample mated against a 316 (lower test piece) stainless steel sample in which the 304 sample was rotated against a stationary 316 sample. This dissimilar sample approach is designed to facilitate future work to identify the mechanisms of material transfer between samples (or otherwise). This would involve local chemical analysis as the two alloys have different chemical compositions [24].

The test pieces themselves are hollow cylinders 20 mm in length where the contacting face is Ø12.7 mm outer diameter (OD) and Ø 6.375 mm inner diameter (ID). Testing was conducted on samples with parallel ground surfaces giving them a surface roughness (Ra) of approximately 0.2–0.4 μm as measured with an Alicona G4 InfiniteFocus optical profilometer. Prior to testing, any burrs were removed using 400 grit silicon carbide paper on the outer and inner diameter perpendicular to the test surface. The surfaces were then cleaned using cotton wool and ethanol.

2.3. Test procedure

Initial tests across a range of loads were conducted to determine the load under which galling started to become much more frequent (Due to limited sample availability, insufficient tests were conducted to allow the G_{50} value as defined in the ASTM standard to be accurately determined). This transition was found to occur at a contact pressure of 5 MPa (between the reported G_{50} values of self-mated 304 and 316 alloys of 4.3 and 7.8 MPa respectively [3,4]). The majority of the tests were subsequently carried out with two nominal contact pressures 5 MPa (0.437 kN) and 50 MPa (4.735 kN).

Tests were conducted to explore the following effects: (i) environmental temperature; (ii) sliding speed; (iii) interruptions during sliding; (iv) sliding distance.

- **Environmental temperature:** Tests with 360° rotation at 5.5 rpm were conducted with a nominal contact pressure of 5 MPa at both room temperature (10 replicate tests) and 100 °C (11 replicate tests).
- **Rotational speed:** Tests with 360° rotation at room temperature were conducted with the two nominal contact pressures and two rotational speeds, with the number of replicate tests as follows: 5 MPa, 5.5 rpm - 10 replicate tests; 50 MPa, 5.5 rpm - 6 replicate tests; 5 MPa, 2.1 rpm - 4 replicate tests; 50 MPa, 2.1 rpm - 5 replicate tests.
- **Interruptions during sliding:** Tests with 360° rotation at 5.5 rpm and at room temperature were conducted under both nominal contact pressures. Each increment of rotation was 90° and between increments, the interruption time was ~5 s. The number of replicate tests in each case was as follows: 5 MPa, uninterrupted - 10 replicate tests; 50 MPa, uninterrupted - 6 replicate tests; 5 MPa, interrupted - 5 replicate tests; 50 MPa, interrupted - 5 replicate tests.
- **Sliding distance:** Room temperature tests with varying degrees of rotation at 5.5 rpm were conducted with a nominal contact pressure of both 5 MPa and 50 MPa. For the tests at 50 MPa, rotations of 90° (6 replicate tests), 180° (8 replicate tests), 270° (3 replicate tests) and 360° (6 replicate tests) were conducted, and in each case, the rotation was uninterrupted. For the tests at 5 MPa, both single rotations (360° - 10 replicate tests) and five rotations (1800° - 3 replicate tests) were conducted. Due to rig constraints, tests with more than a single rotation were interrupted, the samples were disengaged and rotated back to their start position before further rotation was applied.

2.4. Sample characterisation following galling

Following testing, samples were removed and their surfaces visually

inspected for galling, both by eye and via low magnification stereoscopy. The characteristics of galling included concentric striations, severe macroscale surface roughening (where the grinding marks are no longer observed) and/or cold welding of the two samples. The determination of whether a sample has galled or not is not always straightforward. Profilometry has been suggested as a useful additional surface characterization tool [26,27]. Therefore, profiles of the full working surface of selected samples were obtained using an Alicona G4 InfiniteFocus optical profilometer. Maximum height, Sz, (the sum of the maximum peak height and the maximum pit depth) [28] of surfaces were measured both before and after galling testing. ΔSz, the difference in Sz across the whole surface profiles before and after testing, was used as a measure of surface damage.

2.5. Analysis of torque data

The coefficient of friction, μ, in an annular contact can be estimated from the torque and the sample dimensions via the following equation [29]:

$$\mu = \frac{3}{2}\frac{r_2^2 - r_1^2}{r_2^3 - r_1^3}\left(\frac{T}{F_a}\right) \quad (1)$$

where T is the measured torque, r_1 and r_2 are the inner and outer radii respectively of the contacting faces and F_a is the applied normal force. The specimen radii r_1 and r_2 (as per ASTM G196) are 3.1875 mm and 6.3500 mm respectively. It is assumed that the forces are equally distributed with regard to radial position. However, this assumption has limited validity in galling tests as there may be instances where the torque is generated from specific high points on the surfaces with different radial positions. Therefore, this is only an estimate of the coefficient of friction.

3. Results

3.1. Stochastic nature of galling

The stochastic nature of galling was observed in this work, both from the characteristics of the galled samples and from the friction coefficient evolution during the tests (Fig. 3). Under the test conditions selected, the majority of sample pairs tested under a nominal contact pressure of 5 MPa did not exhibit galling damage. The corresponding friction evolution traces are relatively stable (Fig. 3), with some exhibiting a steady increase in coefficient of friction (but not above ~ 0.6) as the rotation proceeded. However, one friction trace (of the eight presented) was very different, exhibiting a rapid rise between a quarter and a half turn to a friction coefficient of above 1.0. Similarly, a variation in behaviour is seen when tests were conducted under the 50 MPa contact pressure. One sample (of the five examined) exhibited a steady and low friction evolution trace whilst all the others exhibited rapid increases in friction associated with galling. It is notable that this absence of galling in the one sample took place under conditions where the nominal contact pressure (50 MPa) is ten times greater than that at which it was deemed that galling was becoming prevalent (5 MPa).

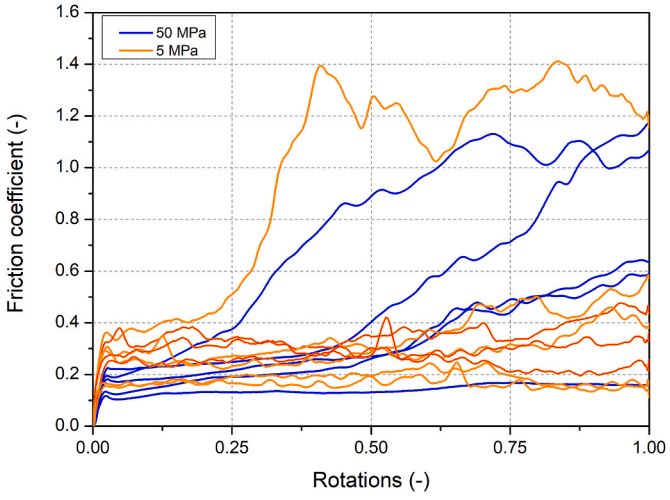

Fig. 3. Evolution of friction coefficient from multiple individual galling tests during a single rotation (360°) at a rotational speed of 5.5 rpm at room temperature under a nominal pressure of both 5 MPa and 50 MPa.

Four illustrative cases which represent the limits of behaviour observed (i.e. samples which both have and have not galled under each of the applied pressures) have been selected and their friction evolution traces are presented in Fig. 4a. In each of the four cases selected, macrographs of the 304 sample surface following the galling tests are presented in Fig. 4b–e. It can be seen that the samples which exhibited clear galling (i.e. large scale surface disruption) (Fig. 4b and d) also exhibited friction evolution traces where high values of coefficient of friction were observed (Fig. 4a). Likewise, in the cases where the coefficient of friction remained low and steady throughout the test (for both contact pressures), no clear evidence of galling was observed on macrographs of the sample surfaces (Fig. 4c and e).

Noting the stochastic nature of galling, the selection of friction coefficient evolution traces to illustrate the effects of changes in the various parameters is not entirely straightforward. The methodology applied in this work was to identify and present the friction coefficient evolution trace corresponding to the median value of μ at the end of the test. We refer to this as the "representative (median)" trace. Whilst this reduces the amount of data presented it provides clarity appropriate for this paper.

3.2. Effect of specimen temperature

Of the ten samples tested at room temperature, one pair exhibited galling and nine did not, whereas all twelve of the samples tested at 100 °C exhibited galling.

Fig. 5 shows the effect of temperature on the evolution of friction coefficient (tests conducted under a nominal applied pressure of 5 MPa) with macrographs of the sample surfaces and their surface profiles being presented in Fig. 6. At room temperature, the friction coefficient remained relatively steady throughout the test and whilst evidence of relative motion could be observed on the 304 sample following testing, this was slight and not deemed to be galling (Fig. 6). In contrast, the evolution of friction coefficient during the test conducted at 100 °C exhibited a rapid increase between 0.25 and 0.5 turns (Fig. 5) and although it fell towards the latter part of the test, it remained at a higher value than at any point in the room temperature test. Clear evidence of galling was observed on the 304 sample tested at 100 °C. The surface profile revealed the formation of a deep trench (~50 μm in depth) with a prow (~70 μm in height) at the head of the trench. The measured ΔSz values at room temperature were 8 μm and 9 μm for the 304 and 316 respectively, whilst at 100 °C, the values of ΔSz were 71 μm and 42 μm for 304 and 316 respectively.

3.3. Effect of sliding speed

Fig. 7 shows the effect of sliding speed on the evolution of friction coefficient during room temperature tests at 5 MPa and 50 MPa. At 5 MPa, the evolution of coefficient of friction remained relatively steady and low at both rotation speeds which is characteristic of an absence of galling. However, at 50 MPa, the evolution of coefficient of friction exhibited a significant increase towards the latter stages of the rotation at both 2.1 rpm and 5.5 rpm, which is characteristic of galling (see Fig. 4). At both applied pressures, the coefficient friction was generally higher with the higher rotational velocity. It is proposed, therefore, that within this range of rotational velocity, the rotational velocity does not

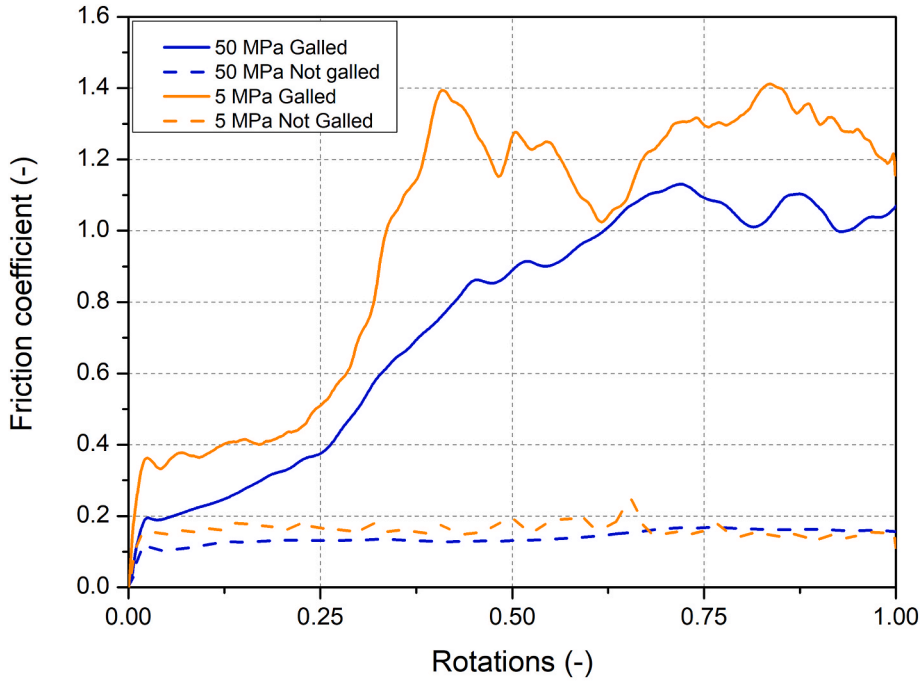

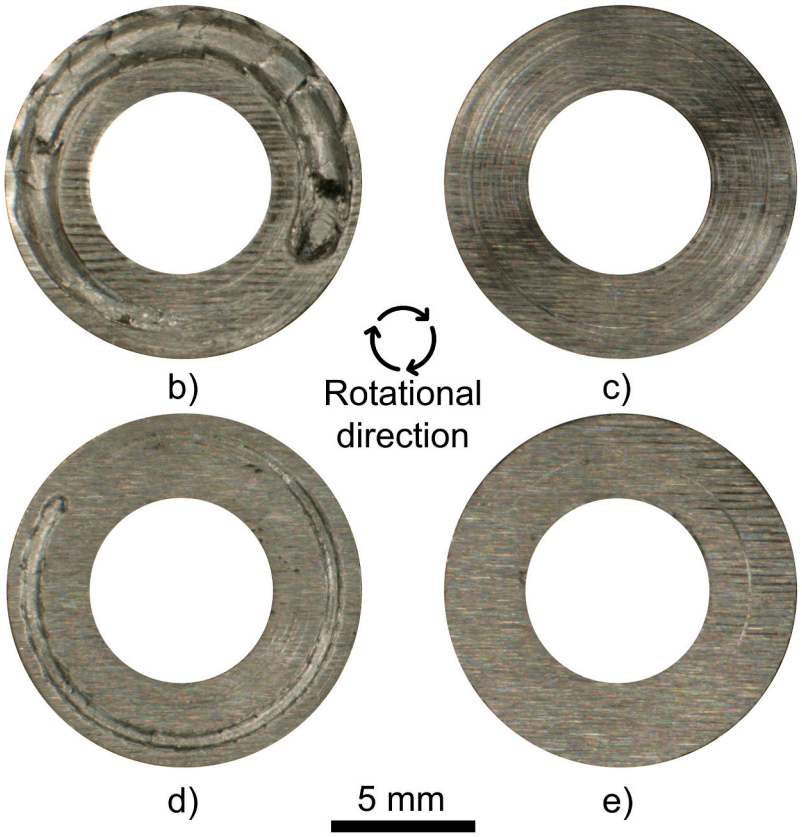

Fig. 4. (a) Evolution of friction coefficient from selected individual galling tests during a single rotation (360°) at a rotational speed of 5.5 rpm at room temperature under a nominal pressure of both 5 MPa and 50 MPa; the samples were selected as the limits of behaviour at each load from the tests presented in Fig. 3. Post-test macrographs of the 304 sample surfaces related to each of the tests presented: (b) 50 MPa - galled; (c) 50 MPa - not galled; (d) 5 MPa - galled; (e) 5 MPa - not galled.

significantly affect the galling behaviour at either of the applied nominal pressures.

3.4. *Effect of interruption in sliding*

Fig. 8 shows the effect of an interruption during a single rotation of sliding on the evolution of friction coefficient during tests conducted

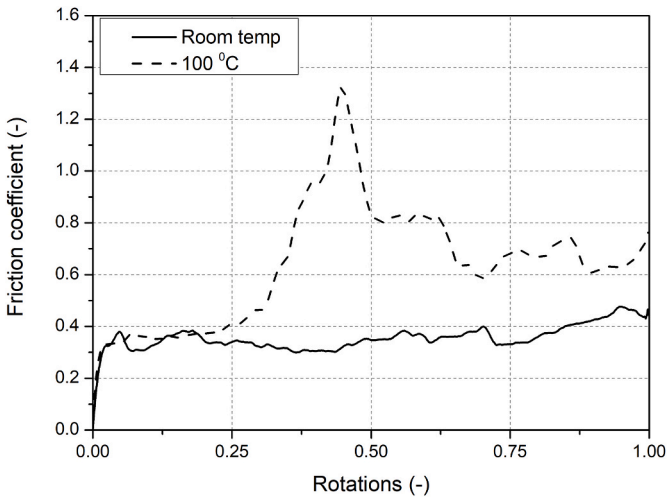

Fig. 5. Evolution of friction coefficient from representative (median) galling tests during a single rotation (360°) at a rotational speed of 5.5 rpm with a nominal contact pressure of 5 MPa at both room temperature and 100 °C.

under nominal applied pressures of both 5 MPa and 50 MPa at room temperature. A significant difference cannot be observed between tests that were interrupted and those that ran continuously, and this was reinforced by observations of the sample surfaces following testing. Irrespective of interruption during rotation, at 5 MPa, galling was not observed and at 50 MPa, galling was observed. This conclusion was reinforced by examination of the wider set of data available in terms of proportions of samples which galled and did not gall. Within the limits of this experimental programme, it is concluded that interruption during testing does not have a significant effect upon galling behaviour.

3.5. *Effect of sliding distance*

Fig. 9 shows the effect of sliding distance on the evolution of friction coefficient during tests conducted under a nominal applied pressure of 50 MPa at room temperature. Macrographs of corresponding 304 alloy sample surfaces and their surface profiles are shown in Fig. 10. All friction coefficient traces follow a similar pattern, with the friction coefficient being low after 0.25 of a rotation, but starting to show a significant increase between 0.25 and 0.5 of a turn.

Fig. 10 shows that there is no evidence of galling after 0.25 turn of sliding, either by visual inspection or by examination of the surface profile. However, clear galling damage is seen after 0.5 turns, with this increasing in severity with subsequent increases in sliding distance. ΔSz as a function of sliding distance for both 304 and 316 specimens is plotted in Fig. 11 (this figure also includes data associated with tests conducted at 5 MPa). To allow a reasonable scale on the graph, the values of ΔSz are not shown for sliding distances of 0.75 and 1 turn at 50 MPa, but it is noted that they are all greater than 400 μm. Values of ΔSz tend to be significantly higher in the softer and less galling resistant 304 stainless steel. After 0.25 turns (where it was deemed that galling had not taken place), ΔSz of the 304 specimen was 21 μm (indicating that some changes to the surface had occurred) whereas after 0.5 turns (where it was deemed that galling had occurred), ΔSz of the 304 specimen had significantly increased to 110 μm.

The effect of sliding distance on the evolution of friction coefficient during tests conducted under the lower nominal applied pressure of 5 MPa at room temperature is presented in Fig. 12 with macrographs of the sample surfaces and their surface profiles shown in Fig. 13. Samples had to be interrupted and repositioned following each full turn (360°) of sliding and this has resulted in clear discontinuities in the friction trace at each complete rotation. The interrupted tests, where repositioning was not required (Fig. 8), did not display discontinuities. The general trend observed in Fig. 12 is that the coefficient of friction increased as the sliding distance increased, although the very high values of coefficient of friction observed for tests conducted at 50 MPa had still not been reached by the end of 5 turns at 5 MPa. Images of the 304 sample surfaces following 1 turn and 5 turns (Fig. 13) show that there was no evidence of galling after 1 turn of sliding, either by visual inspection or by examination of the surface profile. However, clear evidence of galling was observed on the macrograph of the 304 sample after 5 turns, with the surface profile indicating the formation of a deep trench on the sample (~40 μm in depth). Of the three tests conducted with five full rotations), all three exhibited clear visual (and profilometric) evidence

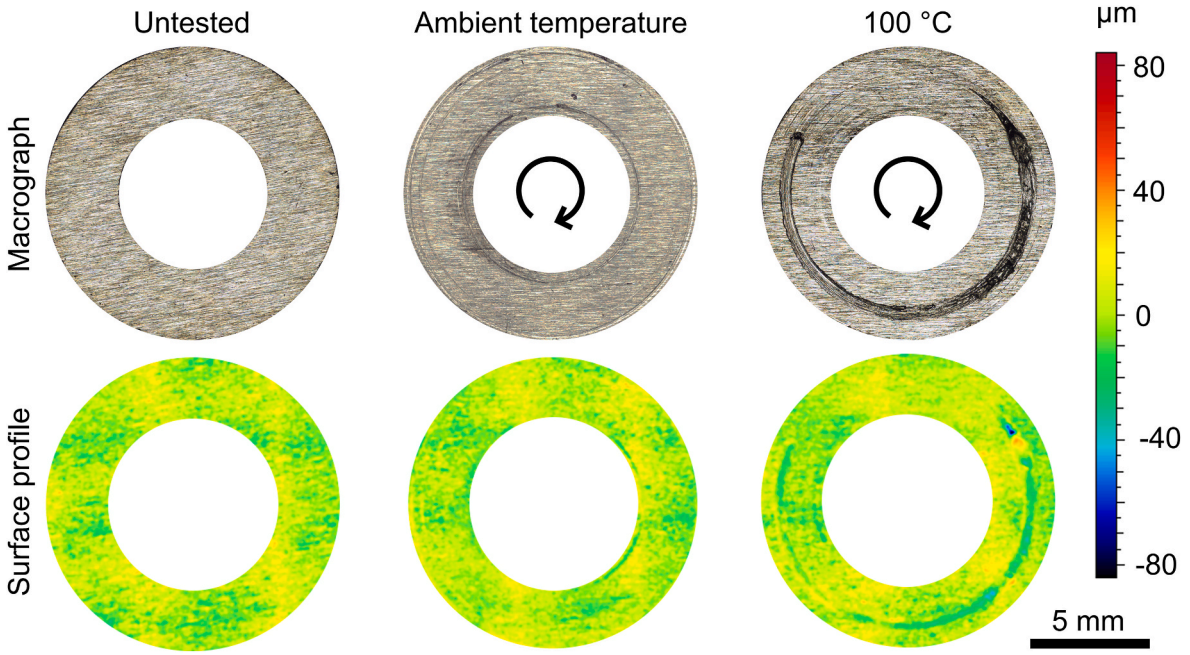

Fig. 6. Optical images and surface profiles of the 304 sample surfaces following galling testing a single rotation (360°) and a rotational speed of 5.5 rpm with a nominal contact pressure of 5 MPa: prior to testing; following testing at room temperature; and following testing at 100 °C.

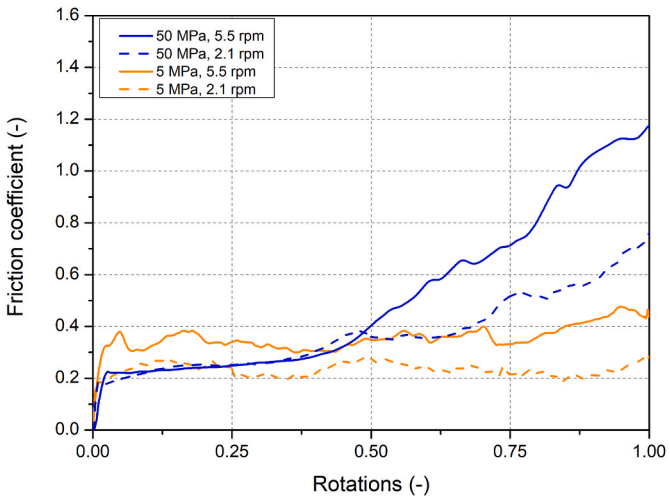

Fig. 7. Plot showing effect of rotational speed (5.5 rpm and 2.1 rpm) on evolution of friction coefficient from representative (median) galling tests during a single rotation (360°) at room temperature with a nominal contact pressure of both 5 MPa and 50 MPa.

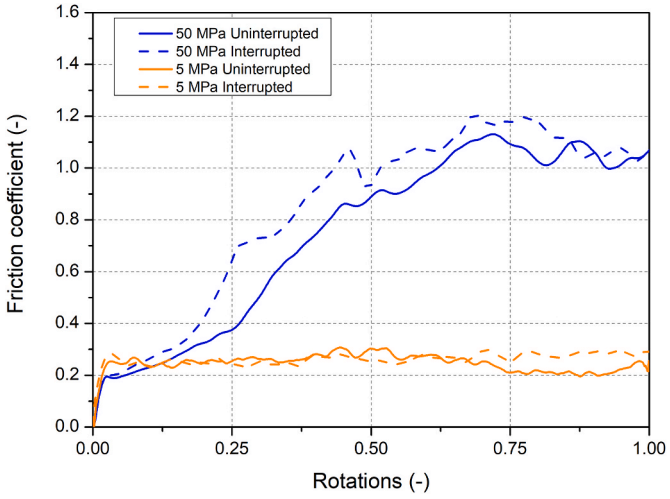

Fig. 8. Plot showing effect of interrupted testing on the evolution of friction coefficient from representative (median) galling tests during a single rotation (360°). Rotational speed of 5.5 rpm at room temperature under nominal pressures of 5 MPa and 50 MPa. Uninterrupted tests were run with a continuous steady rotation; interrupted tests had the rotation stopped at each of (0.25 turn, 0.5 turn, 0.75 turn for ~ 5s before the rotation was continued.

of galling. ΔSz as a function of sliding distance for both the 304 and 316 specimens (Fig. 11) shows that after 5 turns, the samples were assessed as having galled (optical observation) and yet the value of ΔSz for the 304 sample was still only 30 μm.

4. Discussion

The effects of a number of parameters upon the galling of dissimilar 304–316 stainless steel mating pairs have been examined in this work, with the key information available being the evolution of friction coefficient throughout the galling tests along with macrographs and height profiles of the sample surfaces following galling.

The visual examination of specimen surfaces, which allows a determination of galling to be made, is aided by the information regarding surface profiles. However, only the torque measurement provides any information about the development of damage during the galling test

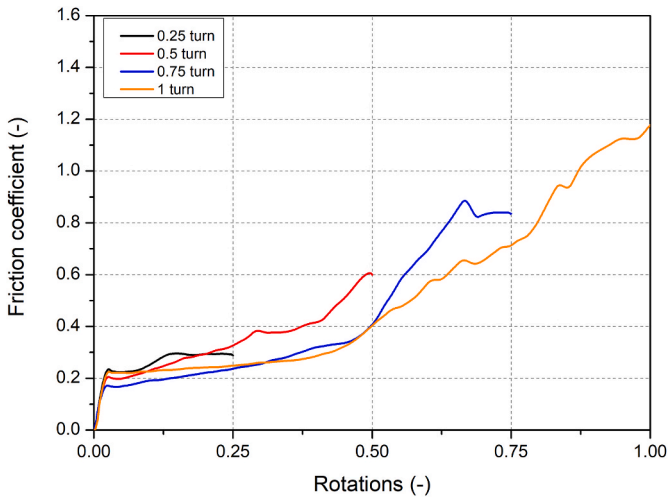

Fig. 9. Effect of sliding distances (0.25 turn, 0.5 turn, 0.75 turn and 1 turn) on evolution of friction coefficient from representative (median) galling tests during rotation at a speed of 5.5 rpm at room temperature under a nominal pressure of 50 MPa.

itself, and it is observed that galling is generally associated both with higher coefficient of friction during the galling test and with higher values of ΔSz. Indeed, as Hummel [23] has argued, changes in measured friction during galling tests may be useful in identifying levels of damage that are being accrued prior to galling being deemed to have occurred. The Sz value may be of use in deciding if galling has occurred in a test (or not) but currently can only be used as supplementary information as the ASTM G196 standard [3] requires that the designation of a galled surface is made on the basis of a visual examination.

The stochastic nature of galling (where the behaviour in tests run under the same conditions can potentially be very different) is a key understanding that underpins the way that the ASTM G196 test standard [3] is constructed, and has been clearly observed in the outcomes of the tests in this work (Figs. 3 and 4). The stochastic nature means that the behaviour of each individual test needs to be understood (and cannot be inferred from a similar test on a similar material pair). The evolution of the friction coefficient through the test is clearly a unique and valuable piece of information in being able to critically interpret and understand galling behaviour.

The galling resistance of the material combination examined in this work fell with an increase in environmental temperature from room temperature (18 °C) to just 100 °C. At the lower temperature, just one out of ten pairs galled with an applied nominal pressure of 5 MPa, whereas at the higher temperature, all the sample pairs tested exhibited galling. This observation is in line with the general understanding of the importance of temperature in determining galling behaviour, and specifically with the work of Harsh et al. [10] where a decrease in the G_{50} value from 12 MPa at room temperature to 2 MPa at 300 °C was observed for self-mated 316 stainless steel pairs. The observation of this high level of sensitivity to rather modest increases in temperature adds weight to the conclusion that, in order for laboratory galling testing to have any validity with regard to behaviour in service, the test temperature is required to match that of the service conditions being considered.

The ASTM G196 standard [3] is much more specific regarding the velocity of rotation that the predecessor G98 standard [7]. However, in line with the modelling predictions of Poole et al. [9] but in contrast to the position taken by Hummel [14], it has been shown in this work that within the limits of this experimental programme, there is no evidence of galling behaviour being sensitive to the sliding velocity. If this were found to be generally the case for other materials, there would be potential for widening the allowed range of velocities under which galling

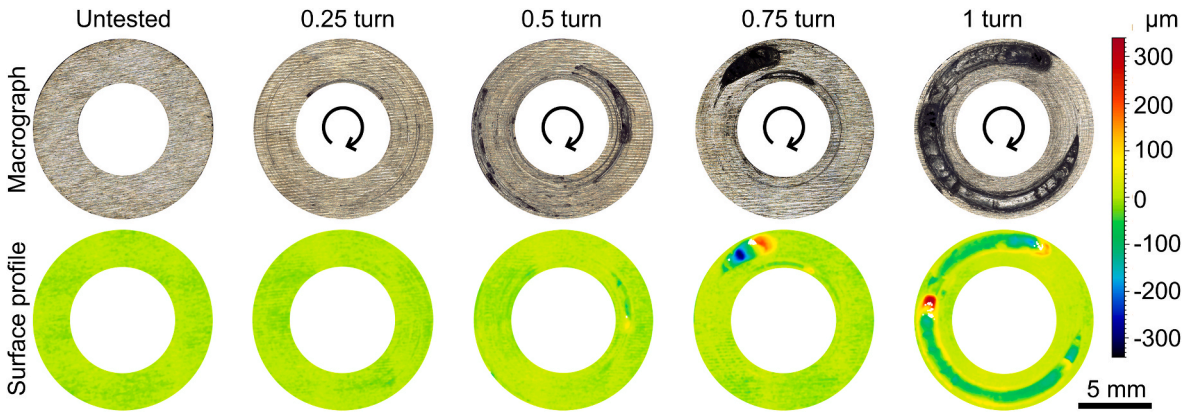

Fig. 10. Optical macrographs (top) and surface profiles (bottom) of the same 304 sample surfaces following galling tests at a speed of 5.5 rpm at room temperature under a nominal pressure of 50 MPa for different sliding distances as indicated.

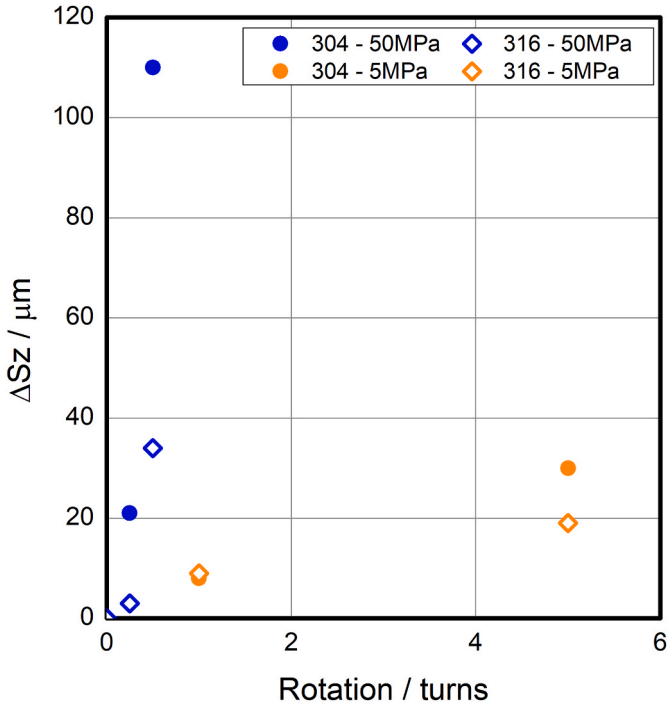

Fig. 11. Increase in maximum height (ΔSz) as a function of sliding distance for both the 304 and the 316 samples following galling testing at a speed of 5.5 rpm at room temperature with nominal contact pressures of 5 MPa and 50 MPa.

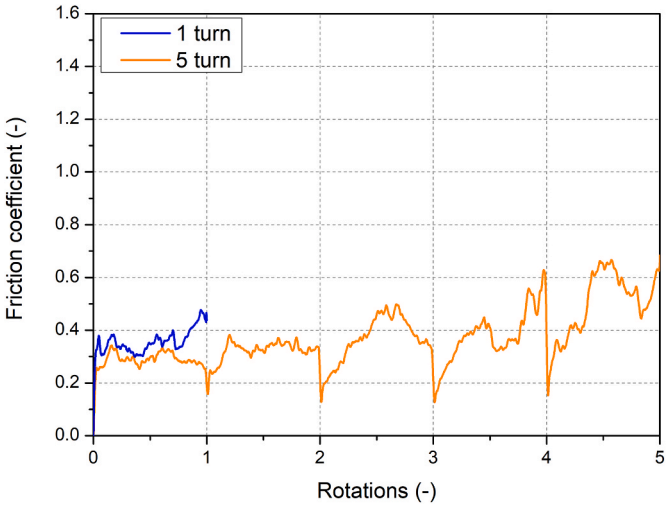

Fig. 12. Evolution of friction coefficient from representative (median) galling tests during rotation at a speed of 5.5 rpm at room temperature under a nominal pressure of 5 MPa for different sliding distances (1 turn and 5 turns). It should be noted that due to rig constraints, the 5 turn test is interrupted.

tests are allowed within the standard. The benefit of such a move would be that it would allow for more experimental facilities to comply with the standard than is currently the case.

In contrast to its narrow specification around sliding velocity, the ASTM G196 standard [3] allows interruption of the rotation to allow for manual devices to be used to rotate the samples in the test, stating: "*Stopping for re-gripping of the turning tool is permitted, but re-gripping should be minimized*". This allowance in the standard is made despite the concerns expressed by Hummel [14] that the galling resistance is likely to be affected by the interruption, and it is perhaps this that resulted in the encouragement in the standard to minimise the number of interruptions. However, in the present work, evidence has not been found that interruption of the test has a measurable influence on the galling behaviour in either galling or non-galling conditions. Our findings therefore support the liberty afforded by the ASTM standard in this regard. One limitation of this study is that it was not possible to maintain the same direction of the lay of the parallel ground surfaces for every test. From the results acquired in the interrupted galling tests, in which the relative orientation of the samples changes at each restart of the test, it is inferred that the direction of the lay has minimal effect on the galling frequency compared to sliding distance and temperature and therefore can be regarded as a second order effect.

There is a general understanding in the literature that (irrespective of the galling test type) as the sliding distance increases, the galling load decreases [15,17]. In this work, it has been seen that at a low applied nominal pressure (5 MPa), galling was rarely seen following a single rotation (360°) whereas after five rotations (1800°), galling was regularly observed. Whilst this galling is clear, it is notable that it resulted in an increase in Sz of only 30 μm on the more galling-prone 304 stainless steel sample. Similarly, under a nominal applied pressure of 50 MPa, in the vast majority of cases, galling was observed after a full turn (360°) and even after half a turn (180°), but was never observed when the sliding distance was shortened to a quarter of a turn (90°). Together, these observations indicate the damage is being accrued in samples even in the period when galling is not observed. Future further work is needed to seek to understand the mechanisms of this damage accumulation. In addition, it is noted that whilst the ASTM standard [3] specifies a single rotation for the galling test, tests with shorter or longer durations may be appropriate depending upon the service conditions that the test is seeking to address. If tests longer than a single rotation are required, it is

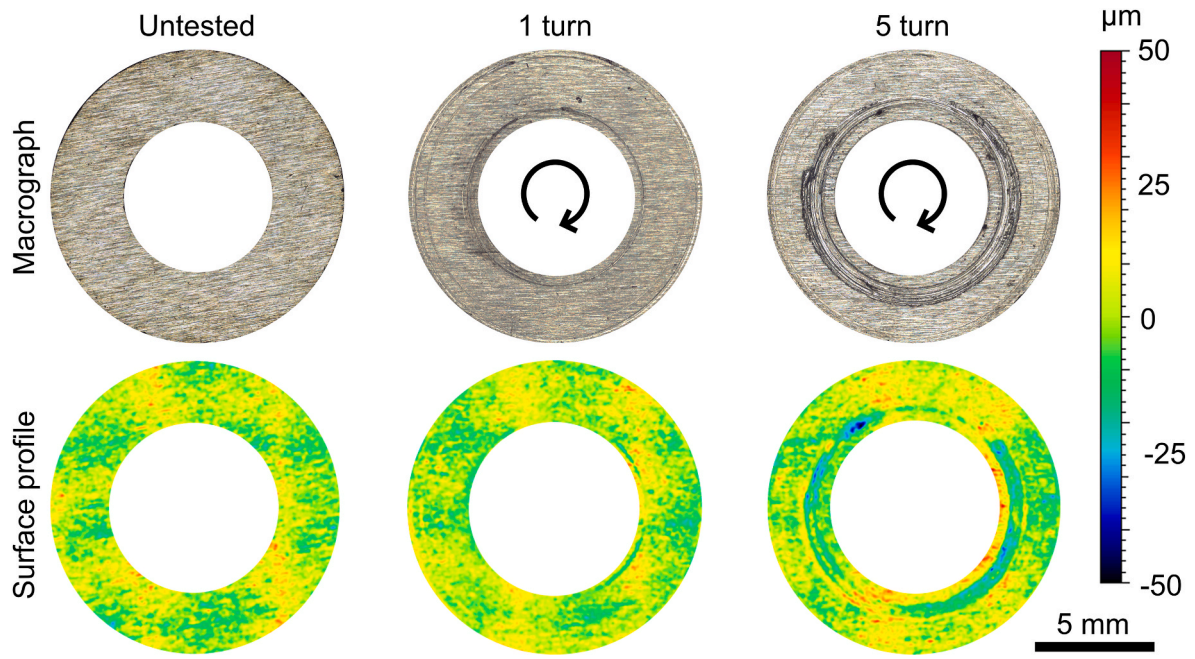

Fig. 13. Optical macrographs (top) and surface profiles (bottom) of the same 304 sample surfaces following galling tests at a speed of 5.5 rpm at room temperature under a nominal pressure of 5 MPa for different sliding distances as indicated.

recommended that an apparatus is employed where multiple turn tests can be conducted without any need for unloading and sample repositioning; in this regard, the test apparatus described by Harsha et al. [8, 10] is preferred to the apparatus described in our present study. More generally, there is a need to be aware of the dependence of galling upon the sliding distance when seeking to apply understanding developed in an ASTM G196 test programme to in-service applications.

5. Conclusions

In this work, the galling behaviour of a 304–316 dissimilar austenitic stainless steel pair was examined in a mechanically driven galling test rig with the capacity to measure frictional coefficient throughout the test. It is shown that even a modest increase in environmental temperature from room temperature to 100 °C results in a significant increase in the tendency to gall. However, the tendency to gall does not appear to be strongly influenced by either the sliding speed during the test or by interruptions during the rotation imposed (within the limits explored by the experimental programme). However, it is seen that galling is sensitive to sliding distance, and that all pairs had an initial period of sliding over which damage is being accrued but in which galling is not observed. Further work is required to understand the nature of this damage accrual in non-galled samples. More generally, the dependence of galling upon sliding distance needs to be considered when applying the results of a laboratory galling test programme to a service environment.

Declaration of competing interest

The authors declare that they have no known competing financial interests or personal relationships that could have appeared to influence the work reported in this paper.

Acknowledgements

The authors would like to thank CNR Services International Ltd., Nottingham, UK. for the design and build of the galling rig and supplying the schematic in Fig. 2. The authors gratefully acknowledge funding from Rolls-Royce plc.

References

[1] B. Podgornik, Adhesive wear failures, J. Fail. Anal. Prev. 22 (2022) 113–138.
[2] I. Hutchings, P. Shipway, Tribology: Friction and Wear of Engineering Materials, Elsevier Science, 2017.
[3] ASTM International, Standard Test Method for Galling Resistance of Material Couples, ASTM G196-08, West Conshohocken, PA, 2021.
[4] S.R. Hummel, J. Helm, Galling50, a stochastic measure of galling resistance, J. Tribol. 131 (2009), 034502/1-3.
[5] E. Rabinowicz, Friction seizure and galling seizure, Wear 25 (1973) 357–363.
[6] P.A. Swanson, L.K. Ives, E.P. Whitenton, M.B. Peterson, A study of the galling of two steels using two test methods, Wear 122 (1988) 207–223.
[7] ASTM International, Standard Test Method for Galling Resistance of Materials, ASTM G98-17, West Conshohocken, PA, 2017.
[8] A.P. Harsha, P.K. Limaye, R. Tyagi, A. Gupta, Development of tribological test equipment and measurement of galling resistance of various grades of stainless steel, J. Tribol. 138 (2016), 024501-1 - 024501-6.
[9] B. Poole, B. Barzdajn, D. Dini, D. Stewart, F.P.E. Dunne, The roles of adhesion, internal heat generation and elevated temperatures in normally loaded, sliding rough surfaces, Int. J. Solid Struct. 185–186 (2020) 14–28.
[10] A.P. Harsha, P.K. Limaye, R. Tyagi, A. Gupta, Effect of temperature on galling behavior of SS 316, 316 L and 416 under self-mated condition, J. Mater. Eng. Perform. 25 (2016) 4980–4987.
[11] R. Komanduri, M.C. Shaw, Galling wear of materials at high speed sliding contact, Wear 33 (1975) 283–292.
[12] F.F. Ling, E. Saibel, Thermal aspects of galling of dry metallic surfaces in sliding contact, Wear 1 (1957) 80–91.
[13] E. van der Heide, D.J. Schipper, Galling initiation due to frictional heating, Wear 254 (2003) 1127–1133.
[14] S.R. Hummel, Elements to improve galling resistance test results using the ASTM G98 method, J. Test. Eval. 39 (2011) 504–507.
[15] S.R. Hummel, B. Partlow, Comparison of threshold galling results from two testing methods, Tribol. Int. 37 (2004) 291–295.
[16] B. Podgornik, S. Hogmark, J. Pezdirnik, Comparison between different test methods for evaluation of galling properties of surface engineered tool surfaces, Wear 257 (2004) 843–851.
[17] L.M. Vilhena, P.V. Antunes, A. Ramalho, Galling characterization for the pair composed by aluminium and M2 steel under dry and lubricated conditions by using load-scanning test method, J. Braz. Soc. Mech. Sci. Eng. 40 (2018). Paper 284.
[18] A. Gåård, P.V. Krakhmalev, J. Bergström, N. Hallbäck, Galling resistance and wear mechanisms – cold work tool materials sliding against carbon steel sheets, Tribol. Lett. 26 (2007) 67–72.
[19] P. Karlsson, P. Krakhmalev, A. Gåård, J. Bergström, Influence of work material proof stress and tool steel microstructure on galling initiation and critical contact pressure, Tribol. Int. 60 (2013) 104–110.
[20] D.-C. Ko, S.-G. Kim, B.-M. Kim, Influence of microstructure on galling resistance of cold-work tool steels with different chemical compositions when sliding against

ultra-high-strength steel sheets under dry condition, Wear 338–339 (2015) 362–371.
[21] M. Boas, A. Rosen, Effect of load on the adhesive wear of steels, Wear 44 (1977) 213–222.
[22] K.G. Budinski, Incipient galling of metals, Wear 74 (1981) 93–105.
[23] S.R. Hummel, An application of frictional criteria for determining galling thresholds in line contact tests, Tribol. Int. 35 (2002) 801–807.
[24] S.R. Rogers, J. Daure, P. Shipway, D. Stewart, D. Dye, Adhesive transfer operates during galling, Scripta Mater. 221 (2022), 114960.
[25] J.L. Daure, M.J. Carrington, D.G. McCartney, D.A. Stewart, P.H. Shipway, Measurement of friction in galling testing – an example of its use in characterising the galling behaviour of hardfacings at ambient and elevated temperature, Wear 476 (2021), 203736.
[26] J.A. Siefert, S.S. Babu, Experimental observations of wear in specimens tested to ASTM G98, Wear 320 (2014) 111–119.
[27] J.L. Andreasen, N. Bay, L. De Chiffre, Quantification of galling in sheet metal forming by surface topography characterisation, Int. J. Mach. Tool Manufact. 38 (1998) 503–510.
[28] BS EN ISO 25178-2:2022, Geometrical Product Specifications (GPS). Surface Texture: Areal. Part 2: Terms, Definitions and Surface Texture Parameters, 2022.
[29] S. Singh, Theory of Machines, Pearson Education India, 2013.